

The Mechanism of Intrinsic Variability in Bright Gravitationally Lensed Quasars at $1 < z < 2$

Luis J. Goicoechea^{1,*}, Vyacheslav N. Shalyapin² and Rodrigo Gil-Merino³

¹Departamento de Física Moderna, Universidad de Cantabria, Avda. de Los Castros s/n, 39005 Santander, Spain

²Institute for Radiophysics and Electronics, National Academy of Sciences of Ukraine, 12 Proskura St., 61085 Kharkov, Ukraine

³Instituto de Física de Cantabria (CSIC-UC), Avda. de Los Castros s/n, 39005 Santander, Spain

Abstract: Taking X-ray/UV/optical observations of local Seyfert nuclei into account, we look for evidence supporting a reverberation scenario in three bright gravitationally lensed quasars at $1 < z < 2$. The analysis is based on the normalized structure function of luminosities at middle UV wavelengths (observer-frame optical bands). We concentrate on tackling two issues: initial logarithmic slope and achromaticity. Due to the presence of significant observational noise in the g -band magnitudes of SBS 0909+532, we cannot prove the achromaticity of the structure function of this double quasar. However, the r -band records of SBS 0909+532 leads to a steep initial growth of the corresponding structure function, which is basically consistent with the traces of reverberation in local Seyfert nuclei (initial slope $\beta \sim 0.7$). The structure function of Q0957+561 is roughly achromatic. Moreover, its initial slope agrees with a $\beta = 0.7$ law. Apart from the structure function analysis, there are complementary observations in favour of a reverberation scenario in Q0957+561. The third object is Q2237+0305. The light curves of its four images incorporate both intrinsic and extrinsic (microlensing) variability, and we are not able to fairly determine an initial intrinsic slope for this quadruple quasar. Finally, we present some ongoing projects to better understand the mechanism of intrinsic variability (rest-frame timescales below 100 d) in gravitationally lensed quasars at $\langle z \rangle \sim 1.5$.

Keywords: Gravitational lensing, quasars, visible, time series analysis, time variability.

1. INTRODUCTION

The UV/optical variability of quasars and Seyfert nuclei is related to violent phenomena occurring in hearts of galaxies and/or properties of intervening media. There are many physical mechanisms that are able to produce UV/optical flares, and the search for the actual mechanism(s) plays a key role in the modern astronomy. Several previous studies focused on the initial logarithmic slope of the structure function, which (structure function) describes typical variabilities at different lags (timescales), e.g., [1]. Measured initial slopes were used to check predictions of possible scenarios of variability, e.g., [2-4]. Although the pioneering effort by [2] showed the potential of the method to decide between the most popular scenarios (accretion disc instabilities and nuclear supernovae explosions), there were important caveats. First, the structure function analysis only incorporated a simple disc-instability model. Accretion disc instabilities were described through the cellular-automaton model [2,5]. However, cellular-automaton simulations neglect hydrodynamical effects, which seem to lead to another kind of flares [6] and a different initial slope of the structure function [7]. Second, the observed structure function included observational noise. This noise has a significant effect on the measured variations at the shortest lags and the measured slope [8].

Local Seyfert nuclei show a variety of initial slopes. The square-root noise-less structure functions¹ over rest-frame lags ≤ 100 d have initial slopes $\beta \sim 0.3-0.8$ [3]. If we concentrate on the sources with the steepest growths (NGC 5548 and NGC 7469), then $\langle \beta \rangle \sim 0.7$ (see Tables 1-2 in [3]). In fact, a $\beta = 0.7$ law works at both UV and optical rest-frame wavelengths. This supports a common variability mechanism at $\lambda \sim 1400 \text{ \AA}$ and $\lambda \sim 5000 \text{ \AA}$. While variable X-ray/EUV irradiation of an accretion disc can account for the similar variability in the UV and optical spectral regions (reverberation scenario [9]), it is difficult to reconcile the observations with accretion disc local instabilities. In the reverberation scenario, the flaring activity at different accretion disc radii (corresponding to different emission wavelengths) is driven by higher energy variations that are produced above the disc plane and near the disc axis, e.g., [10,11]. For NGC 5548 and NGC 7469, Collier & Peterson [3] also obtained that the UV and optical variability timescales agree with each other (see Table 3 in [3]). This last result strengthens the reverberation hypothesis and practically rules out the local disc-instability scenario. Most relevant local timescales $\tau(R)$ are proportional to $(R^3 / GM)^{1/2}$, where M is the mass of the central black hole and $R \propto \lambda^{4/3}$ is the emission radius, e.g., [8] and references

*Address correspondence to this author at the Departamento de Física Moderna, Universidad de Cantabria, Avda. de Los Castros s/n, 39005 Santander, Spain; Tel: +34 942201457; Fax: +34 942201402; E-mail: goicol@unican.es

¹The square root of the structure functions once the observational noise is properly subtracted

therein. Hence, assuming that the involved τ scales as λ^2 , the expected relationship $\tau_{opt} \sim 10\tau_{UV}$ is in clear disagreement with the observed one ($\tau_{opt} \sim \tau_{UV}$). On the other hand, nuclear supernovae explosions and compact supernovae remnants (starburst scenario [12]) produce a variability timescale that does not depend on the wavelength (achromatic behaviour). However, in order to reproduce the observed initial slope of ~ 0.7 , a long timescale of $\tau_{sg} \sim 300$ d must be considered [2]. This long timescale is inconsistent with the observed first flattening of the structure functions at rest-frame lags $\ll 300$ d.

On timescales below 100 d, the optical variations of NGC 5548 are similar to its X-ray variations [13]. Suganuma *et al.* [14] also reported a correlation between the optical and X-ray (2-10 keV) light curves of NGC 5548. They found that the amplitude of the optical fluctuation is much smaller than the amplitude of the higher energy fluctuation, and the optical light curve is delayed (with respect to the X-ray record) by 1-2 d. These results unveil the origin of the optical variability in the Seyfert nucleus (timescales < 100 d): reprocessing of X-ray flares by an accretion disc (the flares are released near the disc axis). If we suppose that an accretion disc is irradiated by an X-ray/EUV source on the disc axis, we should see the inner, hotter part of the accretion disc responds before the outer, cooler parts. The response times at different wavelengths are expected to follow a $\tau \propto \lambda^{4/3}$ law. Observations of NGC 7469 are consistent with this law [15-17], so a reverberation scenario is also favoured in this case. The UV/optical variability of both local Seyfert nuclei (NGC 5548 and NGC 7469) is indeed due to accretion disc reprocessing (see also [18]), which confirms the possible association between this scenario and an achromatic structure function with steep initial slope of ~ 0.7 (see the above paragraph).

Recently, the local quasar MR 2251-178 has been monitored simultaneously in X-rays and optical bands [19]. Arévalo *et al.* [19] reported that the optical events lasting ≤ 100 d are plausibly due to reverberation. Accretion disc reprocessing could also produce the UV/optical variability (on rest-frame timescales ≤ 100 d) of a certain population of non-local quasars. Thus, we propose a structure function analysis to identify possible population members to subsequent simultaneous monitoring at X-ray, UV and optical rest-frame wavelengths. The novel method consists of two steps: (1) construction of the structure function at a given wavelength and determination of its initial slope β , (2) if $\beta \sim 0.7$, comparison with a second structure function at another wavelength.

A main advantage of analysing light curves of gravitationally lensed quasars (GLQs) is that one is able to disentangle intrinsic from extrinsic signal in certain GLQs, e.g., [8,20,21]. While brightness records of non-lensed distant quasars may contain unrecognized extrinsic variations (caused by, e.g., moving compact objects within the intergalactic medium [4]), we can assess the extrinsic variability of certain GLQs and determine their intrinsic

fluctuations (and the corresponding structure functions). Thus, GLQs allow us to fairly study the nature of violent phenomena in distant sources, which very likely arise in the vicinity of a supermassive black hole, e.g., [7,8,22,23]. In this paper, we concentrate on some bright GLQs at $1 < z < 2$ that were observed with the 2-m Liverpool Robotic Telescope (Liverpool Quasar Lens Monitoring - LQLM, e.g., [8,23]) and the 1.3-m Warsaw Telescope (Optical Gravitational Lensing Experiment - OGLE, e.g., [24]).

2. STRUCTURE FUNCTION ANALYSIS

2.1. LQLM Data of SBS 0909+532

The double quasar SBS 0909+532 consists of two images (A and B, with separation of about 1."1.) of the same distant quasar at $z = 1.377$ [25,26]. Both images are relatively bright in the V optical band ($V \sim 17$ -18 mag [27]) and the 2-10 keV X-ray band (global flux of $\sim 3 \times 10^{-13}$ erg s $^{-1}$ cm $^{-2}$ [28]). Lubin *et al.* [29] indicated the possible nature of the main lens galaxy (early-type) and confirmed its redshift ($z_{lens} = 0.830$), while Lehár *et al.* [30] studied the surface brightness distribution of the lens. The optical light curves of the two quasar images were also used to measure the time delay of the system and determine the level of extrinsic variability [8,31]. The LQLM observations indicated that the variability in A and B is basically due to observational noise and intrinsic signal.

From the LQLM r -band brightness records, we constructed the square-root noise-less structure function of the intrinsic luminosity at a rest-frame wavelength $\lambda \sim 2600$ Å (see Fig. 9 in [8]). This showed a steep growth, so here we want to re-discuss the variability structure and to compare it with the $\beta = 0.7$ law. The structure function $SF(L)$ at rest-frame lag $\Delta\tau$ is given by (e.g., [7])

$$SF(L) = (1/2N) \sum_{i,j} [(10^{-0.4m_j} - 10^{-0.4m_i})^2 - \bar{\sigma}_i^2 - \bar{\sigma}_j^2], \quad (1)$$

where m are magnitudes, $\bar{\sigma} = 0.921 \times 10^{-0.4m} \sigma$, σ are photometric uncertainties, and the sum includes N pairs verifying $\tau_j - \tau_i \sim \Delta\tau$. As usual, $L = 10^{-0.4m}$ are monochromatic luminosities in convenient units and τ are rest-frame times. The statistical uncertainties in $SF(L)$, see Eq. (1), are computed as the standard deviations of the means (averaged sums) for the different time lag bins. Thus, the uncertainties are likely underestimated because not all pairs of data in a given bin are independent [3]. We use the function $f = [SF(L)]^{1/2} / \sigma(L)$ instead of $SF(L)$, i.e., we normalize Eq. (1) to the luminosity variance and take the square-root. This normalized structure function was introduced in [7]. Moreover, we only consider rest-frame lags substantially below the rest-frame duration of the A+B combined record, i.e., $\Delta\tau \leq P/4(1+z)$, where $P \sim 500$ d is the observer-frame duration of the combined light curve.

In Fig. (1), using the LQLM r -band observations of SBS 0909+532, we present the normalized structure function at $\lambda \sim 2600$ Å (filled triangles). This is consistent with an initial slope $\beta = 0.7$ (see the dashed line), although the f values have large uncertainties and other slopes cannot be

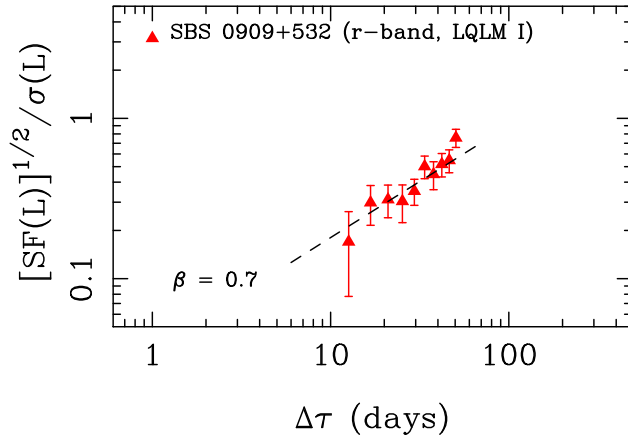


Fig. (1). Normalized structure function of SBS 0909+532 through the LQLM I programme (first phase of the LQLM project) in the r optical band. We describe the variability structure at rest-frame lags ~ 10 -50 d, when the asymptotic behaviour $f = [SF(L)]^{1/2} / \sigma(L) \sim 1$ has not yet been reached. A $\beta = 0.7$ dashed-line is also drawn for comparison purposes.

ruled out. For example, the best-fit line has $\beta \sim 1$ for some lag intervals (see details in [8]). We also observed SBS 0909+532 in the g band (rest-frame wavelength $\lambda \sim 2100$ Å), but the LQLM g -band light curves are excessively noisy. Thus, a detailed comparison of the structure functions at both rest-frame wavelengths is not feasible. In order to properly discuss the multi-wavelength structure function of this promising object, new high signal-to-noise ratio observations in good seeing conditions are required.

2.2. LQLM Data of Q0957+561

Q0957+561 exhibits two images (A and B) of a $z = 1.41$ quasar, with an image separation of about 6" [32]. This double quasar is bright: each image has a visual magnitude $V \sim 17$ mag [27], and the global flux in the 2-10 keV X-ray band is $\sim 2 \times 10^{-13}$ erg s $^{-1}$ cm $^{-2}$ [28]. Optical and near-IR imaging of the system reveals the presence of the main lens galaxy between A and B. The main lens is a giant elliptical (cD) galaxy at $z_{lens} = 0.36$, which is located in the centre of a galaxy cluster [33]. The GLQ is being photometrically monitored in the g and r optical bands with the Liverpool Robotic Telescope. Here we put together several results that were obtained using the first LQLM light curves (LQLM I programme). From these accurate records in both bands, we did not find evidences of extrinsic variability in Q0957+561 [23]. Therefore, this object allows us to carry out a detailed study of its intrinsic fluctuations.

The normalized structure functions, $[SF(L)]^{1/2} / \sigma(L)$ (see subsection 2.1), are shown in Fig. (2) (filled and open circles are associated with g -band and r -band data, respectively). The rest-frame lag intervals are selected like that in Fig. (1), i.e., until one quarter of the rest-frame durations of the whole combined records. As can be seen in Fig. (2), within the error bars, the two growths are consistent with each other. Differences between time coverages, gaps

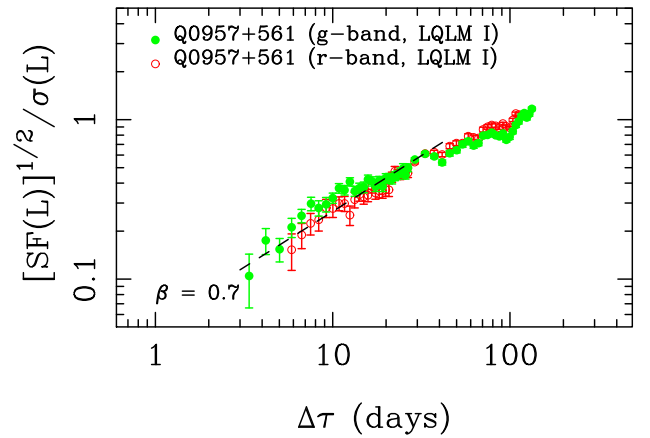


Fig. (2). Normalized structure functions of Q0957+561 through the LQLM I programme in the g and r optical bands. These structure functions of the intrinsic luminosities are accurately described from short rest-frame lags ($\sim 1 - 10$ d) to relatively long rest-frame lags when $f = [SF(L)]^{1/2} / \sigma(L) \sim 1$ (asymptotic behaviour). A $\beta = 0.7$ dashed-line is also drawn for comparison purposes.

and artifacts in the g ($\lambda \sim 2100$ Å) and r ($\lambda \sim 2600$ Å) bands are the most plausible causes of subtle differences between both growths [7]. Apart from this achromaticity, [7] showed that $\beta \sim 0.7$, so a reverberation scenario could explain the variability of Q0957+561. Initial slopes $\beta \leq 0.5$ and $\beta \sim 1$ are not favoured by the LQLM observations (see the dashed line in Fig. 2).

Old records in the g band are also consistent with a $\beta = 0.7$ law [7]. Moreover, the old and LQLM gr light curves of Q0957+561 led to time delays between optical bands that support a reverberation scenario. Collier [22] reported a rest-frame time lag $\Delta\tau_{rg} = 1.4 \pm 0.6$ d (g -band is leading), while Shalyapin *et al.* [23] measured $\Delta\tau_{rg} = 1.7 \pm 0.8$ d. This interband delay of 1-2 d is consistent with that expected from reverberation within an irradiated accretion disc [22]. The presence of an EUV/radio jet (e.g., [34,35]) also suggests the viability of this variability mechanism: EUV/X-ray fluctuations within or close to the jet are reprocessed by rings of the disc (each ring emits light at a certain rest-frame wavelength). Thus, the first GLQ Q0957+561 is an ideal object to future follow-up observations in several spectral regions, including X-ray, UV and optical rest-frame wavelengths.

For an irradiated disc, if the high-energy source is placed on the axis and at a height H_x above the thin disc (with negligible thickness), the temperature at radius R is given by (e.g., [7,36])

$$T(R) = \left[\frac{3GM\dot{M}}{8\pi\sigma R^3} + \frac{(1-A)L_x H_x}{4\pi\sigma(H_x^2 + R^2)^{3/2}} \right]^{1/4}. \quad (2)$$

In Eq. (2), G is the gravitation constant, σ is the Stefan constant, M is the mass of the central black hole, \dot{M} is the mass accretion rate, A is the disc albedo, i.e., the ratio of

reflection to incident high-energy radiation, and L_x is the luminosity of the irradiating source. This Eq. (2) can be rewritten in terms of the standard temperature [37], the irradiation-to-viscosity ratio α_{iv} (α_{iv} in the present paper is IVR in paper [7]) and a geometrical factor $g(R)$, i.e.,

$$T(R) = \left(\frac{3GM\dot{M}}{8\pi\sigma R^3} \right)^{1/4} [1 + \alpha_{iv}g(R)]^{1/4}, \quad (3)$$

where

$$\alpha_{iv} = \frac{2(1-A)L_x H_x}{3GM\dot{M}}, \quad (4)$$

and

$$g(R) = \frac{R^3}{(H_x^2 + R^2)^{3/2}}. \quad (5)$$

We focus on a simple scenario involving a central irradiating source ($H_x \sim R_s$, $R_s = 2GM/c^2$ being the Schwarzschild radius), so $g(R) \sim 1$ and $T(R) \sim [3GM\dot{M}(1 + \alpha_{iv})/8\pi\sigma R^3]^{1/4}$ at practically any radius along the accretion disc ($R \gg H_x$). When a high-energy flare (ΔL_x) occurs in the central region, it propagates out at a speed c and arrives at radius R after a time $\tau \sim R/c$. At this radius R , the temperature rises and the peak emissivity increases [10,16]. Hence, the high-energy flare is reprocessed to roughly produce a fluctuation at $\lambda \sim 0.26[hc/kT(R)]$ (black-body emission peak), where k is the Boltzmann constant and h is the Planck constant. The final $\tau - \lambda$ relationship is

$$\tau \sim 6 \left[\frac{3GM\dot{M}(1 + \alpha_{iv})}{8\pi\sigma c^3} \right]^{1/3} \left(\frac{k\lambda}{hc} \right)^{4/3}. \quad (6)$$

A future multi-wavelength monitoring campaign should be useful to check the feasibility of this $\tau \propto \lambda^{4/3}$ law, as well as to derive physical parameters.

2.3. OGLE Data of Q2237+0305

Q2237+0305 is a quadruply imaged quasar (images A-D) forming a nearly perfect cross [38-40]. The quasar has a redshift of $z = 1.695$, and its four bright images ($V \sim 17-19$ mag [27] and $F_{2-10keV} \sim 4 \times 10^{-13}$ erg s $^{-1}$ cm $^{-2}$ [41]) are located at the central part of a face-on spiral galaxy (lens galaxy) at $z = 0.039$. The OGLE V -band light curves of the quasar images revealed significant extrinsic activity over the past decade [24].

Here, we take the four OGLE V -band records until HJD-2450000 = 4365 (one for each image) to check their structure functions. There was some debate about the right photometric calibration of the OGLE III record of D [42]. According to [42], the OGLE III data of this image are corrected by -0.5 mag. Each light curve of Q2237+0305 covers about 10 years (3700 d), and shows both intrinsic and extrinsic variations. The extrinsic variability is usually

associated with microlensing caused by stars in the lens galaxy bulge. Thus, for each image, we construct the normalized structure function of μL , where μ is the variable microlensing magnification and μL is the microlensed luminosity. The four structure functions appear in Fig. (3). For the A and C images (filled and open circles, respectively), a $\beta = 0.7$ law works surprisingly well at rest-frame lags $\sim 1-70$ d. The situation is different for the B and D images (filled and open triangles, respectively). The structure function of B is consistent with $\beta \sim 0.5$ (1-50 d interval), whereas the structure function of D is characterized by a very initial plateau ($\Delta\tau \sim 1-10$ d) and a slope of ~ 0.5 at $\Delta\tau \sim 10-100$ d. The photometric data of the faintest image D have large uncertainties, so the true (very small) variability of this image on very short time-scales is probably undetectable from its OGLE light curve. Thus, we assume that the plateau is an artifact and the initial slope is $\beta \sim 0.5$.

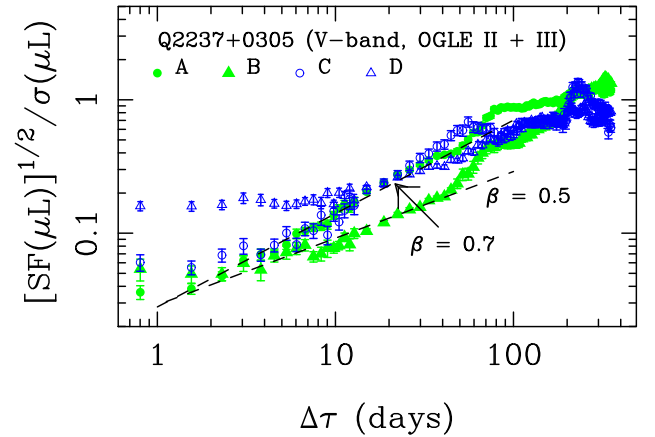


Fig. (3). Normalized structure functions of the four images of Q2237+0305 through the OGLE II+III programmes in the V optical band. We remark that each image of Q2237+0305 varies as consequence of both intrinsic and extrinsic (microlensing) phenomena, and thus, we display the structure function of the microlensed luminosity μL . The rest-frame lag interval is selected like those in Figs. (1-2) (see main text for details).

How can we interpret the results in Fig. (3)? A naive interpretation is as follows: the normalized structure functions of the extrinsically and intrinsically variable quasar Q2237+0305 show a dual behaviour. The $\beta = 0.7$ law works well for two images (A and C) of this quadruple quasar, which seems to indicate that we detect an initial intrinsic slope similar to those in the structure functions of SBS 0909+532 and Q0957+561, i.e., microlensing (extrinsic) variability does not distort the initial growths of both A and C. An initial slope $\beta \sim 0.5$ is clearly seen in the structure functions of the other two images (B and D), so microlensing variability might be the mechanism to flatten their initial growths. However, this attractive interpretation has serious problems and is likely wrong. For example, strong microlensing episodes were observed in the quasar images A and C, e.g., [42,43]. This seems inconsistent with an intrinsic origin for the observed steep slope ($\beta \sim 0.7$). Moreover,

microlensing does not play an important role in the variability of the image D, e.g., [42,43]. Thus, its structure function is expected to be weakly influenced by microlensing. A more plausible alternative is to assume an initial intrinsic slope of ~ 0.5 . This hypothesis agrees with the intrinsic structure function of the GLQ SDSS J1004+4112 at $z = 1.734$ [21], as well as variability studies of some local Seyfert nuclei [3]. The steep slope ($\beta \sim 0.7$) would be related to microlensing variability, in agreement with theoretical predictions by Lewis and Irwin [44]. We note that both interpretations could be partially or totally wrong, since one needs to separate the pure intrinsic variability to properly discuss its structure function. Although Eigenbrod *et al.* [42] have carried out polynomial fits to extract the intrinsic fluctuations, the extraction task is really difficult and uncertain for Q2237+0305. Detailed microlensing simulations for the four images of Q2237+0305 (accounting for the observational sampling and monitoring period) should also help to decide on the pure extrinsic variations and the associated initial slopes, e.g., *see the contribution by Garsden and Lewis in this special volume.*

3. SUMMARY AND ONGOING PROJECTS

The UV/optical variability (on timescales below 100 d) of two well-studied Seyfert nuclei at $z \ll 1$ (NGC 5548 and NGC 7469) very probably represents the response of their gaseous accretion discs to variations in higher energy sources that are located above the disc planes and near the disc axes (reprocessing or reverberation scenario). Both local active galactic nuclei are characterized by an achromatic (square-root noise-less) structure function with initial logarithmic slope $\beta \sim 0.7$, so this achromatic $\beta = 0.7$ law could be related to the reverberation scenario. In this contribution, we propose a structure function analysis to select non-local quasars whose variability is likely due to reverberation within gas discs around supermassive black holes. For a given non-local quasar, the key idea is to construct its structure function at a certain wavelength, and to estimate the corresponding initial slope. If this is $\beta \sim 0.7$, the next step consists of comparing the first variability structure to a second structure function at another wavelength. We focus on three bright GLQs: SBS 0909+532 ($z = 1.377$), Q0957+561 ($z = 1.41$) and Q2237+0305 ($z = 1.695$). The Liverpool Quasar Lens Monitoring (LQLM) light curves of the two first objects exclusively incorporate intrinsic variations, and thus, they allow us to fairly study the nature of the underlying intrinsic signals. The structure function of SBS 0909+532 at a rest-frame wavelength $\lambda \sim 2600 \text{ \AA}$ basically agrees with an initial steep slope of ~ 0.7 . Unfortunately, we are not able to accurately trace the intrinsic variations of SBS 0909+532 at $\lambda \sim 2100 \text{ \AA}$ (observational noise strongly perturbs the LQLM g -band brightness records), so the achromaticity test cannot be done. The LQLM structure functions of the Q0957+561 luminosity at both $\lambda \sim 2100 \text{ \AA}$ and $\lambda \sim 2600 \text{ \AA}$ are similar and consistent with $\beta \sim 0.7$. Thus, Q0957+561 is an excellent candidate object to subsequent simultaneous monitoring at

X-ray, UV and optical rest-frame wavelengths. Apart from the structure function analysis, there are additional observations supporting a reverberation scenario in Q0957+561. With respect to the third object Q2237+0305, the Optical Gravitational Lensing Experiment records of its four images are used to check the influence of extrinsic (microlensing) variations on intrinsic trends. The study of the microlensed luminosity of Q2237+0305 does not permit us to decide on the initial intrinsic slope and the associated variability mechanism.

We have detected a strong activity in Q0957+561 over the last three years. In particular, the g -band flux of its leading image A increased 30% just after a deep minimum, i.e., it changed from $g \sim 17.45$ to $g \sim 17.15$ mag over about 130 days. We have also measured a significant increase ($\sim 20\%$) in the r -band flux of A, which confirms the existence of an optical event [45]. The most recent LQLM observations of A (first semester of 2009) show this event has peaked and later decreased in brightness. As the prominent fluctuation in the optical brightness of A occurred between late 2008 and the middle of 2009, it is expected a similar fluctuation in the light curve of the trailing image B in the first semester of 2010, starting in early February and reaching its maximum in June (taking a time delay of about 14 months into account). Thus, a multiwavelength (X-ray, UV, optical, NIR) follow-up of this system over the next months offers a unique opportunity to fully understand the variability mechanism of a distant quasar: is the optical event (which corresponds to middle UV emission at the redshift of the quasar) triggered (and thus preceded) by another of higher energy?, does the $\tau \propto \lambda^{4/3}$ law work?... We are monitoring this object in the g and r optical bands (LQLM II programme), and planning to get a more complete optical/NIR database (*griz* observations) in 2010. We also plan to obtain NUV frames with the UV/Optical Telescope (UVOT) on board the Swift satellite. These efforts will be complemented with Chandra X-ray observations. The target is visible and observable (3-ks exposures) from January to June 2010. Thus, beginning in mid January, we will obtain 12 epochs of 3 ks each spread relatively uniformly over the first semester of 2010 (about 1 exposure every 15 days). New multiwavelength observations of Q0957+561 are also crucial to close down a 30-year debate on the origin of the short timescale variability in the first GLQ. For example, we could definitively rule out the presence of substantial extrinsic fluctuations produced by collapsed objects in the main lensing galaxy or cosmic strings (*see the contribution by Sazhin et al. in this special volume* for details about effects of cosmic strings).

In 2008 February, we started the second phase of the LQLM project (LQLM II programme). The list of targets includes several GLQs whose images are as bright as or brighter than 19 mag in the r -band (SDSS photometric system). This ongoing programme is providing accurate light curves of GLQs at $1 < z < 2$, so new intrinsic structure functions will be available in a near future. Apart from the LQLM II data, we are also involved in the analysis of

Maidanak brightness records of GLQs. Some examples of these collaborative efforts are [31,46]. Maidanak observations are also providing interband time delays and evidence of reprocessing in GLQs (*see the contribution by Koptelova and Oknyanskij in this special volume*). We are simultaneously preparing programmes to be done with new future facilities. In particular, we belong to the WSO-UV (World Space Observatory-Ultraviolet) Science Working Group in Spain. The WSO-UV is intended to be launched in 2013, and is expected to operate for about 10 years. This space observatory will incorporate an 1.7-m telescope and three UV/optical instruments. The preliminary design can be found in Gómez de Castro *et al.* [47] and on the mission web page [48]. We are mainly involved in the design and simulated (scientific) performance of the instrument ISSIS (Imaging and Slitless Spectroscopy Instrument for Surveys). ISSIS is being developed to carry out UV and optical diffraction limited imaging of astronomical objects (FWHM $\sim 0.''1$), and it will also provide slitless spectroscopic capabilities ($R \sim 300$, including the availability of masks). The key idea is an instrument that will have two channels: High Sensitivity Channel (HSC; 1200-2000 Å) and Channel for Surveys (CfS; 1200-6000 Å). The CfS will be based on a CCD camera with a pixel scale of 0.''05 and a FOV of $3.''4 \times 3.''4$. This CfS will permit us to study the variability of typical GLQs ($z \sim 1.5$) at rest-frame wavelengths $\lambda \sim 480$ -2400 Å i.e., from the extreme UV to the middle UV.

ACKNOWLEDGEMENTS

We thank A. Ullán and several members of the Maidanak collaboration for interesting discussions, support and sharing information. We use datasets taken from our LQLM I Data-Tools Release on the Gravitational LENSES and DARK MATTER (GLEN DAMA) web site (<http://grupos.unican.es/glendama/>) and the Optical Gravitational Lensing Experiment (OGLE) web site (<http://ogle.astrouw.edu.pl/>), and we are grateful to C. Moss for guidance in the preparation of the robotic monitoring project with the Liverpool Telescope, and the OGLE team for doing a public database. This research has been financially supported by the Spanish Department of Science and Innovation grant AYA2007-67342-C03-02 and University of Cantabria funds.

REFERENCES

[1] Simonetti JH, Cordes JM, Heeschen DS. Flicker of extragalactic radio sources at two frequencies. *Astrophys J* 1985; 296: 46-59.
 [2] Kawaguchi T, Mineshige S, Umemura M, Turner EL. Optical variability in active galactic nuclei: starbursts or disk instabilities?. *Astrophys J* 1998; 504: 671-69.
 [3] Collier S, Peterson BM. Characteristic ultraviolet/optical timescales in active galactic nuclei. *Astrophys J* 2001; 555: 775-85.
 [4] Hawkins MRS. Variability in active galactic nuclei: confrontation of models with observations. *MNRAS* 2002; 329: 76-86.
 [5] Mineshige S, Ouchi BN, Nishimori H. On the generation of 1/f fluctuations in X-rays from black-hole objects. *PASJ* 1994; 46: 97-105.
 [6] Manmoto T, Takeuchi M, Mineshige S, Matsumoto R, Negoro H. X-ray fluctuations from locally unstable advection-dominated disks. *Astrophys J* 1996; 464: L135-L138.
 [7] Goicoechea LJ, Shalyapin VN, Gil-Merino R, Ullán A. Structure function of the UV variability of Q0957+561. *Astron Astrophys* 2008; 492: 411-47.

[8] Goicoechea LJ, Shalyapin VN, Koptelova E, Gil-Merino R, Zheleznyak AP, Ullán A. First robotic monitoring of a lensed quasar: intrinsic variability of SBS 0909+532. *New Astron* 2008; 13: 182-93.
 [9] Collin-Souffrin S. On the origin of the optical and UV continuum in active galactic nuclei. *Astron Astrophys* 1991; 249: 344-50.
 [10] Collier S, Horne K, Wanders I, Peterson BM. A new direct method for measuring the Hubble constant from reverberating accretion discs in active galaxies. *MNRAS* 1999; 302: L24-L28.
 [11] Sergeev SG, Doroshenko VT, Golubinskiy YuV, Merkulova NI, Sergeeva EA. Lag-luminosity relationship for interband lags between variations in B, V, R, and I bands in active galactic nuclei. *Astrophys J* 2005; 622: 129-35.
 [12] Aretxaga I, Cid Fernandes R, Terlevich R. QSO variability: probing the starburst model. *MNRAS* 1997; 286: 271-83.
 [13] Czerny B, Schwarzenberg-Czerny A, Loska Z. The power density spectrum of NGC 5548 and the nature of its variability. *MNRAS* 1999; 303: 148-56.
 [14] Suganuma M, Yoshii Y, Kobayashi Y, *et al.* Reverberation measurements of the inner radius of the dust torus in nearby Seyfert 1 galaxies. *Astrophys J* 2006; 639: 46-63.
 [15] Wanders I, Peterson BM, Alloin D, *et al.* Steps toward determination of the size and structure of the broad-line region in active galactic nuclei. XI. Intensive monitoring of the ultraviolet spectrum of NGC 7469. *Astrophys J* 1997; 113: 69-88.
 [16] Collier SJ, Horne K, Kaspi S, *et al.* Steps toward determination of the size and structure of the broad-line region in active galactic nuclei. XIV. Intensive optical spectrophotometric observations of NGC 7469. *Astrophys J* 1998; 500: 162-72.
 [17] Kriss GA, Peterson BM, Crenshaw DM, Zheng W. A high signal-to-noise ultraviolet spectrum of NGC 7469: new support for reprocessing of continuum radiation. *Astrophys J* 2000; 535: 58-72.
 [18] Chesnok NG, Sergeev SG, Vavilova IB. Optical and X-ray variability of Seyfert galaxies NGC 5548, NGC 7469, NGC 3227, NGC 4051, NGC 4151, Mrk 509, Mrk 79, and Akn 564 and quasar 1E 0754. *Kinematics and Physics of Celestial Bodies* 2009; 25: 107-13.
 [19] Arevalo P, Uttley P, Kaspi S, Breedt E, Lira P, McHardy IM. Correlated X-ray/optical variability in the quasar MR2251-178. *MNRAS* 2008; 389: 1479-88.
 [20] Kundic T, Turner EL, Colley WN *et al.* A robust determination of the time delay in 0957+561A,B and a measurement of the global value of Hubble's constant. *Astrophys J* 1997; 482: 75-82.
 [21] Fohlmeister J, Kochanek CS, Falco EE, Morgan CW, Wambsgans J. The rewards of patience: an 822 day time delay in the gravitational lens SDSS J1004+4112. *Astrophys J* 2008; 676: 761-6.
 [22] Collier S. Evidence for accretion disc reprocessing in QSO 0957+561. *MNRAS* 2001; 325: 1527-32.
 [23] Shalyapin VN, Goicoechea LJ, Koptelova E, Ullán A, Gil-Merino R. New two-colour light curves of Q0957+561: time delays and the origin of intrinsic variations. *Astron Astrophys* 2008; 492: 401-10.
 [24] Udalski A, Szymanski MK, Kubiak M, *et al.* The optical gravitational lensing experiment: OGLE-III long term monitoring of the gravitational lens QSO 2237+0305. *Acta Astronomica* 2006; 56: 293-305.
 [25] Kochanek CS, Falco EE, Schild R, Dobrzycki A, Engels D, Hagen HJ. SBS 0909+532: a new double gravitational lens or binary quasar? *Astrophys J* 1997; 479: 678-83.
 [26] Oscoz A, Serra-Ricart M, Mediavilla E, Buitrago J, Goicoechea LJ. Support for the gravitational lens interpretation of SBS 0909+532. *Astrophys J* 1997; 491: L7-L9.
 [27] Kochanek CS, Falco EE, Impey C, *et al.* CASTLES Gravitational Lens Data Base, 2009 Available at: <http://www.cfa.harvard.edu/castles/>
 [28] Chartas G. X-ray observations of gravitationally lensed quasars: evidence for a hidden quasar population. *Astrophys J* 2000; 531: 81-94.
 [29] Lubin LM, Fassnacht CD, Readhead ACS, Blandford RD, Kundic T. A Keck survey of gravitational lens systems. I. Spectroscopy of SBS 0909+532, HST 1411+5211, and CLASS B2319+051. *Astron J* 2000; 119: 451-9.
 [30] Lehár J, Falco EE, Kochanek CS, *et al.* Hubble Space Telescope observations of 10 two-image gravitational lenses. *Astrophys J* 2000; 536: 584-605.

- [31] Ullán A, Goicoechea LJ, Zheleznyak AP, *et al.* Time delay of SBS 0909+532. *Astron Astrophys* 2006; 452: 25-35.
- [32] Walsh D, Carswell RF, Weymann RJ. 0957+561A,B: twin quasistellar objects or gravitational lens? *Nature* 1979; 279: 381-4.
- [33] Young P, Gunn JE, Kristian J, Oke JB, Westphal JA. The double quasar Q0957+561 A,B - A gravitational lens image formed by a galaxy at $z = 0.39$. *Astrophys J* 1980; 241: 507-20.
- [34] Garrett MA, Calder RJ, Porcas RW, King LJ, Walsh D, Wilkinson PN. Global VLBI observations of the gravitational lens system 0957+561A,B. *MNRAS* 1994; 270: 457-64.
- [35] Hutchings JB. Ultraviolet structure in the lensed QSO 0957+561. *Astron J* 2003; 126: 24-8.
- [36] Cackett EM, Horne K, Winkler H. Testing thermal reprocessing in active galactic nuclei accretion discs. *MNRAS* 2007; 380: 669-82.
- [37] Shakura NI, Sunyaev RA. Black holes in binary systems. Observational appearance. *Astron Astrophys* 1973; 24: 337-55.
- [38] Huchra J, Gorenstein M, Kent S, *et al.* 2237 + 0305: A new and unusual gravitational lens. *Astrophys J* 1985; 90: 691-6.
- [39] Yee HKC. High-resolution imaging of the gravitational lens system candidate 2237+030. *Astron J* 1988; 95: 1331-9.
- [40] Schneider DP, Turner EL, Gunn JE, Hewitt JN, Schmidt M, Lawrence CR. High-resolution CCD imaging and derived gravitational lens models of 2237+0305. *Astron J* 1988; 95: 1619-28.
- [41] Fedorova EV, Zhdanov VI, Vignali C, Palumbo GGC. Q2237+0305 in X-rays: spectra and variability with XMM-Newton. *Astron Astrophys* 2008; 490: 989-94.
- [42] Eigenbrod A, Courbin F, Sluse D, Meylan G, Agol E. Microlensing variability in the gravitationally lensed quasar QSO 2237+0305 = the Einstein Cross. I. Spectrophotometric monitoring with the VLT. *Astron Astrophys* 2008; 480: 647-61.
- [43] Shalyapin VN, Goicoechea LJ, Alcalde D, Mediavilla E, Muñoz JA, Gil-Merino R. The nature and size of the optical continuum source in QSO 2237+0305. *Astrophys J* 2002; 579: 127-35.
- [44] Lewis GF, Irwin MJ. The statistics of microlensing light curves - II. Temporal analysis. *MNRAS* 1996; 283: 225-40.
- [45] Goicoechea LJ, Shalyapin VN. A prominent fluctuation in the optical brightness of Q0957+561A and prediction of the Q0957+561B optical variability in the first semester of 2010. 5 October 2009: Available from: <http://www.astronomerstelegam.org/?read=2228>
- [46] Shalyapin VN, Goicoechea LJ, Koptelova E, *et al.* Microlensing variability in FBQ 0951+2635: short-time-scale events or a long-time-scale fluctuation? *MNRAS* 2009; 397: 1982-9.
- [47] Gómez de Castro AI, Shustov B, Sachkov M, Kappelmann N, Huang M, Werner K. The space telescope for ultraviolet astronomy WSO-UV. In: Diego JM, Goicoechea LJ, González Serrano JI, Gorgas J, Eds. *Highlights of Spanish astrophysics V*. Berlin: Springer 2010; p. 219.
- [48] WSO-UV (World Space Observatory-Ultraviolet) Available at: <http://wso.inasan.ru/>

Received: October 02, 2009

Revised: December 03, 2009

Accepted: January 30, 2010

© Goicoechea *et al.*; Licensee *Bentham Open*.

This is an open access article licensed under the terms of the Creative Commons Attribution Non-Commercial License (<http://creativecommons.org/licenses/by-nc/3.0/>) which permits unrestricted, non-commercial use, distribution and reproduction in any medium, provided the work is properly cited.